JOURNAL OF BACTERIOLOGY, Feb. 1994, p. 848–860
0021-9193/94/$04.00+0

Vol. 176, No. 3

Isolation of Two Physiologically Induced Variant Strains of *Bacillus stearothermophilus* NRS 2004/3a and Characterization of Their S-Layer Lattices

MARGIT SÁRA,* DIETMAR PUM, SETA KÜPCÜ, PAUL MESSNER, AND UWE B. SLEYTR

Zentrum für Ultrastrukturforschung und Ludwig Boltzmann-Institut für Molekulare Nanotechnologie, Universität für Bodenkultur, A-1180 Vienna, Austria

Received 3 August 1993/Accepted 25 November 1993

During growth of *Bacillus stearothermophilus* NRS 2004/3a in continuous culture on complex medium, the chemical properties of the S-layer glycoprotein and the characteristic oblique lattice were maintained only if glucose was used as the sole carbon source. With increased aeration, amino acids were also metabolized, accompanied by liberation of ammonium and by changes in the S-layer protein. Depending on the stage of fermentation at which oxygen limitation was relieved, two different variants, one with a more delicate oblique S-layer lattice (variant 3a/V1) and one with a square S-layer lattice (variant 3a/V2), were isolated. During the switch from the wild-type strain to a variant or from variant 3a/V2 to variant 3a/V1, monolayers of two types of S-layer lattices could be demonstrated on the surfaces of single cells. S-layer proteins from variants had different molecular sizes and a significantly lower carbohydrate content than S-layer proteins from the wild-type strain did. Although the S-layer lattices from the wild-type and variant strains showed quite different protein mass distributions in two- and three-dimensional reconstructions, neither the amino acid composition nor the pore size, as determined by permeability studies, was significantly changed. Peptide mapping and N-terminal sequencing results strongly indicated that the three S-layer proteins are encoded by different genes and are not derived from a universal precursor form.

Crystalline bacterial cell surface layers (S layers) can now be considered one of the most common surface structures in prokaryotic cells. S layers have been identified on more than 400 organisms of every taxonomic group of walled bacteria and represent an almost universal feature of archaea. The occurrence of S layers on bacteria from all phylogenetic branches and from quite different natural habitats indicates that they must fulfill a broad spectrum of functions (for reviews, see references 4 to 6, 15, 18, 19, 27, and 36 to 38). The general assumption that S layers endow the cell with a selection advantage in competitive habitats is supported by the observation that they are frequently lost upon prolonged cultivation under optimal laboratory conditions.

As described in previous reports (25, 39), S layers from *Bacillus stearothermophilus* strains isolated from extraction plants in beet sugar factories showed a considerable degree of heterogeneity in lattice type, lattice constant, molecular sizes of S-layer subunits, and presence of covalently bound carbohydrate residues. Despite these differences, S layers of all strains investigated so far were permeable by proteins with molecular weights of up to 30,000, indicating that a limiting pore size could be advantageous for these thermophilic organisms (31–33).

Physiologically, *B. stearothermophilus* strains are capable of oxidatively degrading a broad spectrum of sugars. Under oxygen-limited conditions, their metabolism switches to mixed fermentation in which alcohols and organic acids are formed (23, 40, 42). Since *B. stearothermophilus* strains are highly auxotrophic, they must be supplied with most amino acids and vitamins. Therefore, they are usually grown on complex, not very well-defined, media supplemented with yeast extract and peptone. Depending on the composition of the medium and the rate of aeration, different metabolic pathways leading to quite different degradation products can be induced (10, 23, 40, 42). Detailed studies on the relationship between the physiology and morphology of *B. stearothermophilus* strains have also shown that the structure and composition of the cell wall can be influenced by growth conditions (17).

With several *B. stearothermophilus* strains we demonstrated that the chemical and morphological properties of their S layers were preserved only if growth conditions resembled those of the natural habitat from which the strains had originally been isolated. For example, if oxygen limitation on a complex medium was relieved during growth in continuous culture, reproducible changes in the molecular sizes of the S-layer subunits and the lattice properties occurred. In this article, we describe the isolation and characterization of two physiologically induced variant strains with different S-layer proteins originating from *B. stearothermophilus* NRS 2004/3a.

MATERIALS AND METHODS

Bacterial strain, growth in continuous culture, and isolation of the variant strains. *B. stearothermophilus* NRS 2004/3a was kindly provided by F. Hollaus (Österreichisches Zuckerforschungs-Institut, Tulln, Austria). The strain was grown in 50 ml of SVIII medium (3) in 300-ml shaking flasks at 57°C to mid-exponential growth phase (25). The bacterial suspension (400 ml) was used as an inoculum for 8 liters of SVIII medium sterilized in a 10-liter Braun fermentor (Braun, Melsungen, Germany). Before inoculation, 50 ml of a sterile glucose solution containing a total of 9.6 g of glucose and with a final glucose concentration of 1.2 g per liter of SVIII medium was pumped into the fermentor. All fermentations were performed at 57°C and a stirring speed of 300 rpm. The pH was kept at 7.2 by adding either 1 N NaOH or 2 N H_2SO_4. The optical density

* Corresponding author. Mailing address: Zentrum für Ultrastrukturforschung, Universität für Bodenkultur, Gregor-Mendelstr. 33, A-1180 Vienna, Austria. Phone: 1/47 654 /2208.

at 600 nm (OD_{600}) of the bacterial suspension was measured with a Beckman spectrophotometer (model 25). At the end of the exponential growth phase or when glucose had been completely metabolized, the continuous culture was started with a dilution rate of 0.10 h^{-1}. When bacteria were grown under oxygen-limited conditions, the aeration rate was kept at 0.5 liter of air per min. To change from oxygen-limited to non-oxygen-limited conditions, the aeration rate was increased in steps from 0.5 to 5.0 liters of air per min. If fermentation was started under non-oxygen-limited conditions, the aeration rate was 5.0 liters of air per min. The glucose and ammonium concentrations in the medium were determined with a test kit for glucose (catalog no. 315-100; Sigma, Munich, Germany) or test sticks for ammonium (Merck 10024-0001). For controlling the homogeneity of the culture during the fermentation, 10-ml samples of the bacterial suspension were taken from the fermentor at different phases. Subsequently, aliquots were plated on SVIII agar or subjected to sodium dodecyl sulfate-polyacrylamide gel electrophoresis (SDS-PAGE) and freeze-etching of whole cells, as previously described (25). Single cell colonies that did not look like those present in the inoculum were used for freeze-etching and SDS-PAGE. Isolated variants were subsequently grown on SVIII agar or in shaking flasks as described for the inoculum.

Resistance of whole cells to muramidases. The resistance of the wild-type and variant strains to lysozyme and mutanolysin (both from Sigma) was determined as described in a previous report (25).

Preparation of cell wall fragments and S-layer self-assembly products. Preparation of cell wall fragments from whole cells was done as previously described (35), except that whole cells were broken by ultrasonification under conditions described previously (25). The purity of the cell wall fragments was checked by SDS-PAGE.

For producing S-layer self-assembly products, the S-layer protein from cell wall fragments was extracted with guanidinium hydrochloride (GHCl) (5 M GHCl in 50 mM Tris-HCl buffer [pH 7.2]) for 2 h at 20°C. After centrifugation for 20 min at 40,000 × *g* at 20°C, most of the supernatant was dialyzed against distilled water at 4°C for at least 48 h. Portions (1 to 2 ml) of the GHCl extracts were dialyzed against either a KCl solution (20 mM in distilled water) or a $CaCl_2$ solution (10 mM in distilled water) at 20°C. Samples from all preparations were examined by negative staining, which was done as previously described (25). The S-layer protein obtained after dialysis against distilled water was recovered by centrifugation of the suspensions at 40,000 × *g* for 20 min, and clear supernatants were discarded. Subsequently, 5 ml of the GHCl solution was added to 100 mg of the wet pellet containing S-layer proteins, and GHCl extracts were stirred for 20 min at 20°C. GHCl extracts were then centrifuged at 40,000 × *g* for 30 min at 20°C, and clear supernatants were again dialyzed against distilled water for 48 h at 4°C. The suspensions were lyophilized, and the purity of S-layer proteins was checked by SDS-PAGE.

Image processing. Micrographs were selected with an optical diffractometer for subsequent computer image processing when several high-resolution spots were found beyond a 1/2.5 nm^{-1} threshold. Electron micrograph negatives were digitized with a flat-bed scanner (Elscript 400; ATH, Munich, Germany) with raster spacing corresponding to 0.6 nm at the specimen level. Digitized data (512*512 pixel and 1024*1024 pixel) were Fourier filtered by a peak-profile fitting procedure (termed Deltafilter) as previously described (20). One-sided filtering of superimposed lattices was used to obtain single-layer amplitudes and phases of double-layer self-assembly products of the wild-type strain. Symmetry-related pairs were complex averaged. For three-dimensional reconstructions, several tilt series with different orientations of the tilt axis against the lattice orientation were used (five tilt series for the oblique lattice of the wild-type strain, eight tilt series for the oblique lattice of variant 3a/V1, and six tilt series for the square lattice of variant 3a/V2; all with a tilting range of ±60°C). Procedures based on programs written at the Medical Research Council, Cambridge, United Kingdom (2) were used to obtain a set of three-dimensional structure factors. Backtransformation and determination of threshold values for the data were done as described previously (2, 11). In addition, results from permeability experiments were used to find threshold values which provided valuable information on pore size (29). The three-dimensional models were represented by a surface-shading algorithm as described by Saxton (34).

Chemical characterization of the S-layer proteins. The molecular weights of S-layer proteins were determined on SDS-polyacrylamide gels by using the proteins in a high-molecular-weight protein kit (Sigma) as standards. Protein bands were made visible by the Coomassie R250 staining procedure or the silver staining method (28a). Glycoproteins were either directly visualized on SDS-polyacrylamide gels by the periodate-Schiff staining procedure or were made visible after electroblotting to nitrocellulose membranes and staining with the Boehringer Mannheim DIG glycan detection kit (14). Amino acid analysis was done after hydrolyzing proteins in 6 N HCl for 16 h at 110°C on a Biotronik LC 3000 analyzer (Biotronik, Maintal, Germany). Norleucine was used as the internal standard. Colorimetric estimations of total sugars were performed by the orcinol-H_2SO_4 method (12). Amino sugars were analyzed by a modified version of the assay developed by Rondle and Morgan (30).

Pronase digestion. Lyophilized S-layer proteins were digested with pronase E (Serva, Heidelberg, Germany) as previously described (24). The reaction mixture was purified by a combination of gel permeation chromatography on Bio-Gel P-4 and Bio-Gel P-100 (Bio-Rad Laboratories, Richmond, Calif.) and cation-exchange chromatography on Dowex 50W-X8 H^+ resin (Bio-Rad) as previously described (24). Monosaccharides in glycopeptides were determined after hydrolysis with 2.5 M trifluoroacetic acid at 110°C for 6 h by high-performance anion-exchange chromatography with pulsed amperometric detection (HPAEC-PAD) on a Dionex series DX-300 HPLC system equipped with a CarboPac PA-1 column (Dionex Corp., Sunnyvale, Calif.). Amino sugars were quantified after hydrolysis in 6 N HCl at 110°C for 6 h either on the Biotronik LC 3000 amino acid analyzer or by HPAEC-PAD.

Peptide mapping. Endoproteinase Glu-C (*Staphylococcus aureus* V8 protease; Sigma P-8400) was used for proteolytic cleavage of purified S-layer proteins from the wild-type strain and variants. For this purpose, 500 μg of S-layer proteins was dissolved in 300 μl of SDS solution (0.2% in 0.1 M Tris-HCl buffer [pH 7.8]). Proteins were denatured by heating for 5 min at 100°C. After the solutions were cooled down to 37°C, 50 μg of endoproteinase Glu-C was added to each sample and the samples were incubated for 60 min at 37°C (41). The reaction was finally stopped by adding 5 μl of mercaptoethanol and heating at 100°C for 5 min. Subsequently, samples were subjected to SDS-PAGE performed as previously described (22) using a 10% separation gel. Protein and glycoprotein bands were made visible as described above.

N-terminal sequencing. S-layer proteins (100 to 200 pmol) were dissolved in 20- to 60-μl samples of a solution of 1% SDS, 5% trifluoroacetic acid, and distilled water and used for

N-terminal sequencing, which was done on a reversed-phase high-pressure liquid chromatography (HPLC) system (Applied Biosystems) with a PTH-RP C18 column.

Permeability studies. Permeability properties of S-layer lattices were determined after depositing native cell wall fragments on a microporous support, cross-linking the S-layer protein with glutaraldehyde, and degrading the peptidoglycan-containing layer with lysozyme. The detailed procedure is described in previous reports (31, 33). For determining the rejection characteristics of such S-layer membranes, disks with a diameter of 25 mm were punched out of the membranes and inserted into 10-ml ultrafiltration cells (Amicon type 8010). The permeability studies were carried out as follows. First, 0.4 to 0.7 mg of the test proteins (see Table 6) was dissolved per milliliter of distilled water. The feed solution (4 ml) was concentrated by a factor of 4 at a pressure of 2×10^5 Pa at 20°C and a stirring speed of 500 rpm. The protein concentrations in the feed solution, filtrate, and retentate were determined at 280 nm in a Hitachi spectrophotometer (model U-2000). Rejection coefficients (given as percentile rejection [see Table 6]) were calculated according to the following equation used for batch ultrafiltration procedures (33): $R = (\log c_r - \log c_0)/\log n$, where R is the rejection coefficient, c_r is the concentration in the retentate, c_0 is the concentration in the feed solution, and n is the concentration factor.

RESULTS

Isolation of two variants with different S-layer proteins from continuous culture. The S-layer protein from *B. stearothermophilus* NRS 2004/3a cells used as the inoculum for the fermentor could be separated on SDS-polyacrylamide gels into four bands with apparent molecular weights of 96,000, 119,000, 147,000, and 170,000 (Fig. 1B, lane 1). As previously reported (21, 28, 39), except for the 96,000-molecular-weight protein band, all others could be stained with periodate-Schiff reagent, indicating that they are glycosylated. Detailed structural analyses of the carbohydrate residues of this S-layer glycoprotein have been performed (8, 28). In freeze-etched preparations, whole cells showed the oblique S-layer lattice characteristic of the wild-type strain, with lattice constants of $a = 11.6$ nm, $b = 9.4$ nm, and $\gamma = 78°C$ (see Fig. 2a).

In the initial phase of fermentation, cells were grown under oxygen-limited conditions achieved with an aeration rate of 0.5 liter of air per min (Fig. 1A; Table 1). The OD_{600} of the bacterial suspension increased to 1.45 within 2 h after inoculation. Since at this stage glucose was completely metabolized, continuous culture was started with a dilution rate of 0.10 h^{-1} (Table 1; Fig. 1). In order to keep the pH constant at 7.2, alkali had to be added to the culture, indicating that organic acids had been produced. During the next 2 h, the OD_{600} increased to 1.67 but decreased continuously to 1.23 in the following 14 h. It can be assumed that inhibition of bacterial growth was caused by fermentation products produced under oxygen-limited conditions (1). Samples which were taken 4 and 18 h after inoculation and plated on SVIII agar showed that the culture was homogeneous, since only one colony type that was transparent and 3 mm in diameter was observed. The wild-type strain colonies are hereafter referred to as colony type I. In freeze-etched preparations, whole cells taken from the fermentor showed the oblique S-layer lattice characteristic of the wild-type strain (see Fig. 2a). SDS extracts from the biomass yielded a pattern on SDS-polyacrylamide gels that was identical to that observed for the inoculum (Fig. 1B, lanes 2 and 3).

Eighteen hours after inoculation, the aeration rate was increased to 1.0 liter of air per min, and the OD_{600} of the suspension increased from 1.23 to 1.76 in the next 4 h. As shown in Table 1, under these conditions the culture was still oxygen limited. In contrast to the first phase of fermentation with an aeration rate of 0.5 liter of air per min, the pH of the suspension now remained constant without the addition of alkali. Since glucose was completely metabolized under these conditions and qualitative determination of ammonium gave positive results, it was concluded that equimolar amounts of acid and ammonium were produced. As previously described (10), the production of ammonium by *B. stearothermophilus* strains indicates that oxidative degradation of amino acids was occurring. Liberation of ammonium is caused by deamination reactions before ketoic acids are utilized as carbon sources. Samples taken from the fermentor 1 h after the aeration rate was increased to 1.0 liter/min still showed no changes in the S-layer protein pattern on SDS-polyacrylamide gels. However, when cells were freeze-etched, the oblique S-layer lattice characteristic of the wild-type strain (Fig. 2a) was interrupted in some areas by patches of granular structure (Fig. 2b). Four hours after the aeration rate had been increased, the oblique S-layer lattice of the wild-type strain had completely disappeared. Most of the cells were covered with patches of a more delicate oblique lattice with lattice constants of $a = 9.9$ nm, $b = 7.6$ nm, and $\gamma = 81°$. The crystalline areas were separated by granular regions (Fig. 2c). Samples plated on SVIII agar showed that at least 90% of the colonies had a diameter of approximately 1.5 mm (colony type II) and were therefore significantly smaller than those of the wild-type strain (colony type I). In freeze-etched preparations, cells of these smaller colonies were completely covered with the altered oblique lattice. SDS extracts from biomass taken from the continuous culture at sampling stage 4 (Fig. 1A) revealed a major protein band with a molecular weight of 97,000 on SDS-polyacrylamide gels (Fig. 1B, lane 4), which corresponded exactly to the major protein band observed in SDS extracts from the smaller colonies (type II).

Increasing the aeration rate from 1.0 to 5.0 liters of air per min relieved oxygen limitation (Fig. 1A; Table 1), which led to an increase in the OD_{600} of the cell suspension from 1.84 to 2.64 in the next hour. Quantitative measurements confirmed that glucose had been completely metabolized. Since immediately after the aeration rate was increased the culture required the addition of acid to maintain the pH at 7.2, it was concluded that larger amounts of amino acids were metabolized at this phase. At the end of continuous culture, which was 36 h after inoculation (Fig. 1A), only small colonies (type II) could be observed on SVIII agar plates. Biomass harvested at this time yielded a distinct protein band with a molecular weight of 97,000 on SDS-polyacrylamide gels (Fig. 1B, lane 6) which could not be stained by the periodate-Schiff staining procedure. As shown by freeze-etching, whole cells were still completely covered with the S-layer lattice originally induced by increasing the aeration rate (Fig. 2d). The variant strain isolated from the fermentor under non-oxygen-limited conditions that exhibited the oblique lattice with lattice constants of $a = 9.9$ nm, $b = 7.6$ nm, and $\gamma = 81°$ will hereafter be referred to as variant 3a/V1.

If fermentation of the wild-type strain was started with an aeration rate of 5.0 liters of air per min, the OD_{600} of the suspension increased to 1.55 within 90 min after inoculation (Fig. 3a; Table 2). Since glucose was completely metabolized, the continuous culture was started with a dilution rate of 0.10 h^{-1}. Samples taken from the fermentor already showed two types of colonies. Approximately 90% of the colonies resembled the wild-type strain (colony type I). The other colonies were somewhat larger and more elevated and will hereafter be

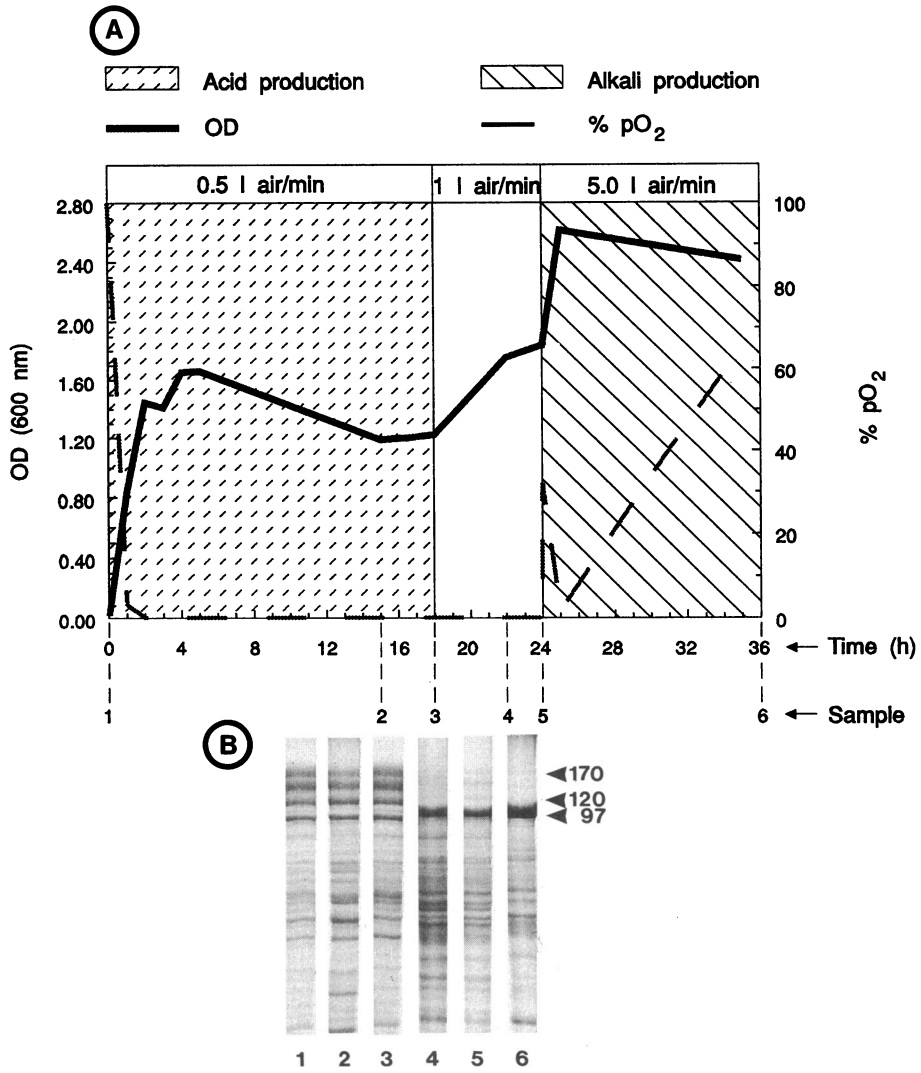

FIG. 1. Protocol of the fermentation of *B. stearothermophilus* NRS 2004/3a in continuous culture (A) and SDS-PAGE patterns of SDS extracts of cell samples grown under different conditions (B). The majority of the protein bands characteristic for the cells used as inoculum and the S-layer protein bands could be preserved only under oxygen-limited conditions (lanes 1 to 3). If the aeration rate was increased in steps (A), variant strain 3a/V1, with distinctly different protein bands and with an S-layer protein with an apparent molecular weight of 97,000, evolved (lanes 4 to 6). Values to the right of panel B are molecular weights (in thousands). pO_2, partial O_2 pressure.

referred to as colony type III. SDS-PAGE of cells at this phase showed that the 147,000- and 170,000-molecular-weight S-layer glycoprotein bands were now more pronounced than they were in the inoculum (Fig. 3B, lanes 1 and 2). Ninety minutes after the start of continuous culture, the OD_{600} of the suspension which produced acid all the time had increased to approximately 2.0. Since in the following intermediate state glucose was completely metabolized while the pH of the culture remained constant without addition of acid or alkali, it was concluded that because of the high aeration rate, amino-group-containing compounds were utilized as carbon sources in addition to glucose. Four hours after inoculation, acid had to be added to the culture to keep the pH at 7.2. At this phase, the OD_{600} of the suspension had increased to approximately 2.5. Samples taken for SDS-PAGE revealed that the original 119,000-molecular-weight glycoprotein band observed for the wild-type strain had split into two bands (Fig. 3B, lane 4), and only the lower-molecular-weight one gave a positive periodate-Schiff reaction (not shown). One hour later, a protein band with an apparent molecular weight of 120,000 was the most prominent band (Fig. 3A, lane 5). The intensities of all other S-layer protein bands characteristic for the cells from the inoculum had decreased considerably. Freeze-etched preparations from samples taken 4 and 5 h after inoculation revealed both cells with the characteristic oblique S-layer lattice of the wild-type strain and cells with many irregularly structured areas on their surface (Fig. 4a and b). Additionally, areas showing a square S-layer lattice with a lattice constant of 13.6 nm had appeared (Fig. 4b). On some cells both types of S-layer lattices could be detected in a monomolecular layer (Fig. 4c), demonstrating that single cells were capable of producing and exporting two different types of S-layer proteins. At an OD_{600} of approximately 2.2 (Fig. 3B, sample 4), 90% of the colonies on SVIII agar plates belonged to colony type I, characteristic of the wild-type strain, but this portion decreased to less than 10% (Fig. 3B, sample 6) once the suspension had reached an

TABLE 1. Growth of *B. stearothermophilus* NRS 2004/3a in continuous culture under oxygen-limited and non-oxygen-limited conditions[a]

Time (in h)	Sample no.	OD_{600}	Aeration rate (liters of air/min)	% pO_2	Required for constant pH
0	1	0.02	0.5	100.0	
1		0.84	0.5	32.0	Alkali
2*		1.45	0.5	0.0	Alkali
4		1.67	0.5	0.0	Alkali
15	2	1.19	0.5	0.0	Alkali
18	3	1.23	0.5	0.0	Alkali
18		1.23	1.0	0.0	
22	4	1.76	1.0	0.0	
24	5	1.84	1.0	0.0	
24		1.84	5.0	32.0	Acid
25		2.64	5.0	1.8	Acid
36	6	2.42	5.0	65.5	Acid

[a] Fermentations were carried out on SVIII medium with 1.2 g of glucose per liter at 300 rpm and 57°C. The aeration rate was increased in steps from 0.5 liter of air per min to the final value of 5.0 liters of air per min. The asterisk indicates when continuous culture was started with a dilution rate of 0.10 h^{-1}.

OD_{600} of about 2.9. In freeze-etched preparations, cells of colony type III exhibited only the square S-layer lattice, with a lattice constant of 13.6 nm (Fig. 4d). SDS extracts of cells from these colonies yielded a major S-layer protein band with an apparent molecular weight of 120,000 on SDS-polyacrylamide gels which did not stain by the periodate-Schiff procedure. Finally, 12 h after inoculation, the culture contained only cells with the square S-layer lattice (Fig. 4d) corresponding to the 120,000-molecular-weight protein band on SDS-polyacrylamide gels (Fig. 3B, lane 7). This isolate was termed variant 3a/V2. SDS extracts from cells taken from the fermentor 10 h later yielded two major protein bands on SDS-polyacrylamide gels with apparent molecular weights of 120,000 and 97,000 (Fig. 3B, lane 8). At this stage, colony types II and III could be observed on SVIII agar plates in approximately equal proportions. In freeze-etched preparations, cells with the square S-layer lattice characteristic of variant 3a/V2 and cells with the delicate oblique lattice characteristic of variant 3a/V1 were observed. In some cases both types of S-layer lattices were detected on the surfaces of single cells (Fig. 4e). Finally, at the end of continuous culture, only cells characteristic of variant 3a/V1 were present in the fermentor (Fig. 4f), indicating that

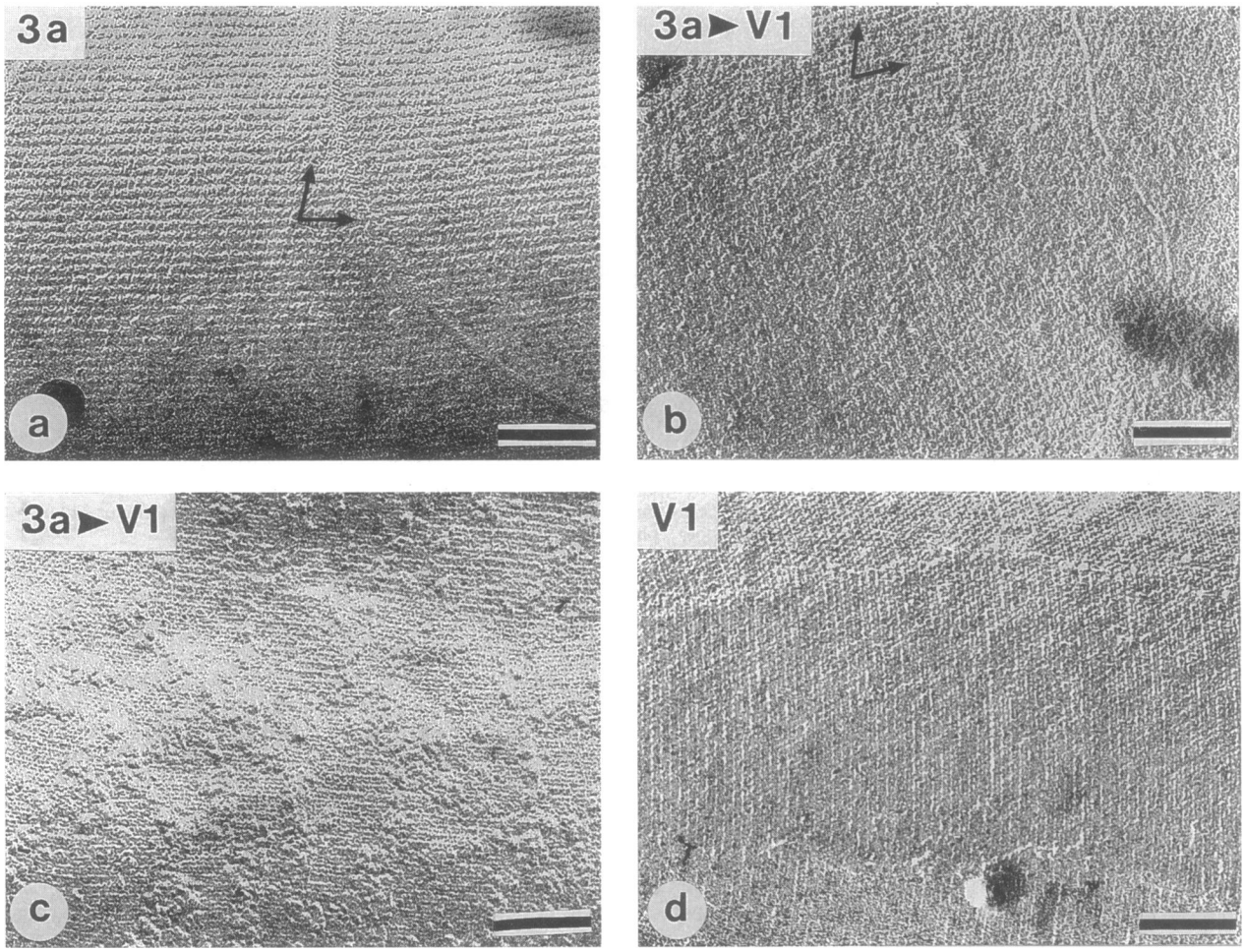

FIG. 2. Freeze-etched preparations of whole cells harvested at different sampling stages of the continuous culture shown in Fig. 1. The wild-type strain *B. stearothermophilus* NRS 2004/3a had an oblique S-layer lattice with constants of a = 11.6 nm, b = 9.4 nm, and γ = 78° (a). When oxygen limitation of the culture was relieved (corresponding to samples 3 to 6 in Fig. 1A), amorphous regions appeared on the cell surface (b). Finally, in addition to the granular areas, an oblique lattice with different lattice constants could be detected (c). At the end of fermentation (corresponding to sample 6), cells were completely covered with the new oblique lattice characteristic of variant 3a/V1 (d). Bars, 100 nm.

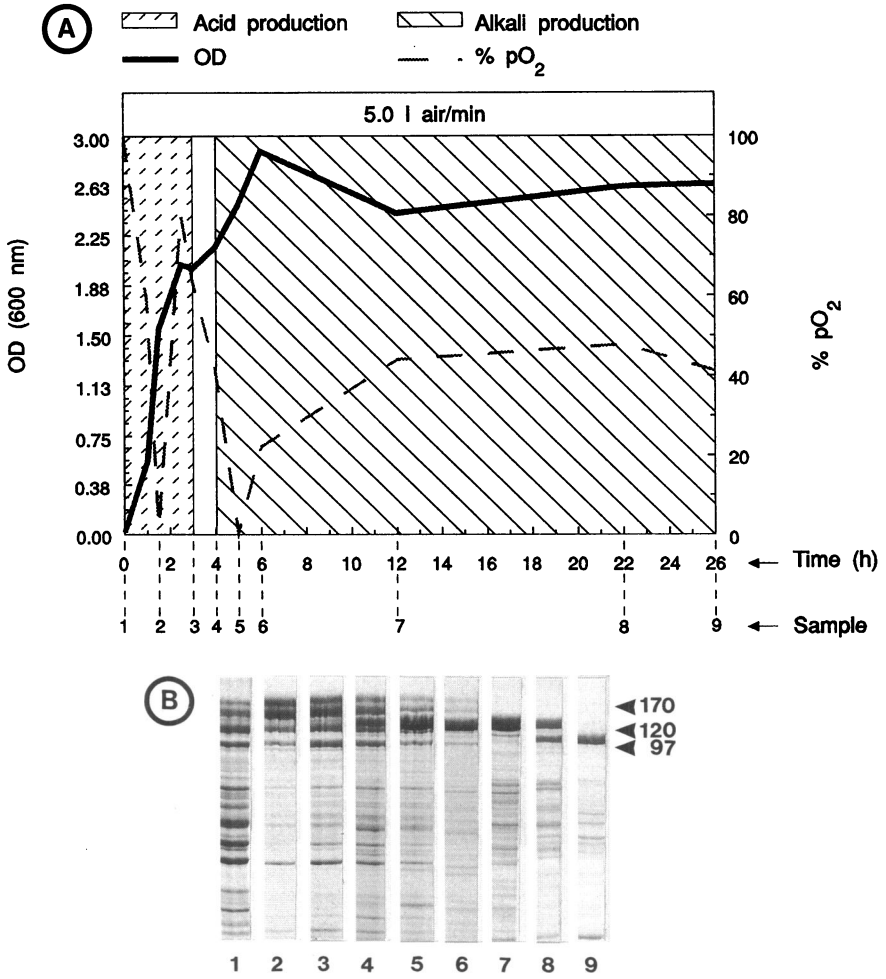

FIG. 3. Protocol of the fermentation of *B. stearothermophilus* NRS 2004/3a in continuous culture which was started under oxygen-saturated conditions (A) and SDS-PAGE patterns of SDS extracts of cell samples harvested at distinct stages (B). Several protein bands characteristic for cells used as the inoculum and the S-layer protein (lane 1) changed rapidly under oxygen-saturated conditions (lanes 2 to 7). The S-layer protein from the variant strain 3a/V2 (lane 7) had an apparent molecular weight of 120,000. During prolonged cultivation in continuous culture under oxygen saturation, variant 3a/V2 switched to variant 3a/V1 (lanes 8 and 9), revealing the characteristic apparent molecular weight of 97,000 for the S-layer protein. Values to the right of panel B are molecular weights (in thousands). pO_2, partial O_2 pressure.

TABLE 2. Growth of *B. stearothermophilus* NRS 2004/3a in continuous culture under non-oxygen-limited conditions[a]

Time (in h)	Sample no.	OD_{600}	% pO_2	Required for constant pH
0	1	0.02	100.0	
1		0.57	58.5	Alkali
1.5*	2	1.55	1.3	Alkali
2.5		2.04	80.2	Alkali
3	3	2.01	63.6	
4	4	2.17	41.0	Acid
5	5	2.48	0.4	Acid
6	6	2.89	22.4	Acid
12	7	2.42	44.0	Acid
22	8	2.62	47.8	Acid
26	9	2.64	41.2	Acid

[a] Fermentations were carried out on SVIII medium with 1.2 g of glucose per liter at 300 rpm and 57°C, and an aeration rate of 5.0 liters of air per min was used. The asterisk indicates when continuous culture was started with a dilution rate of 0.10 h^{-1}.

this variant was the most stable form on complex medium under non-oxygen-limited conditions.

Growth of variant strains in continuous culture under oxygen-limited conditions. For investigating whether the S-layer proteins of the two isolated variant strains were stable under growth conditions where the glycosylated S-layer protein of the wild-type strain could be preserved, variants were grown in continuous culture under oxygen-limited conditions. Single cell colonies from SVIII agar plates were used as the inoculum. The homogeneity of the inoculum was examined by plating suspension samples on SVIII agar, by SDS-PAGE of whole-cell extracts, and by freeze-etching of whole cells. For variant 3a/V2, all colonies were identical. Freeze-etching showed that the cells were completely covered with the square S-layer lattice. By contrast, for variant 3a/V1 at least two types of colonies differing slightly in their transparency could be distinguished on SVIII agar plates. Nevertheless, SDS extracts from all colonies yielded identical patterns on SDS-polyacrylamide gels and showed an S-layer protein band with an apparent molecular weight of 97,000. Since in freeze-etched preparations cells from all colonies revealed the oblique

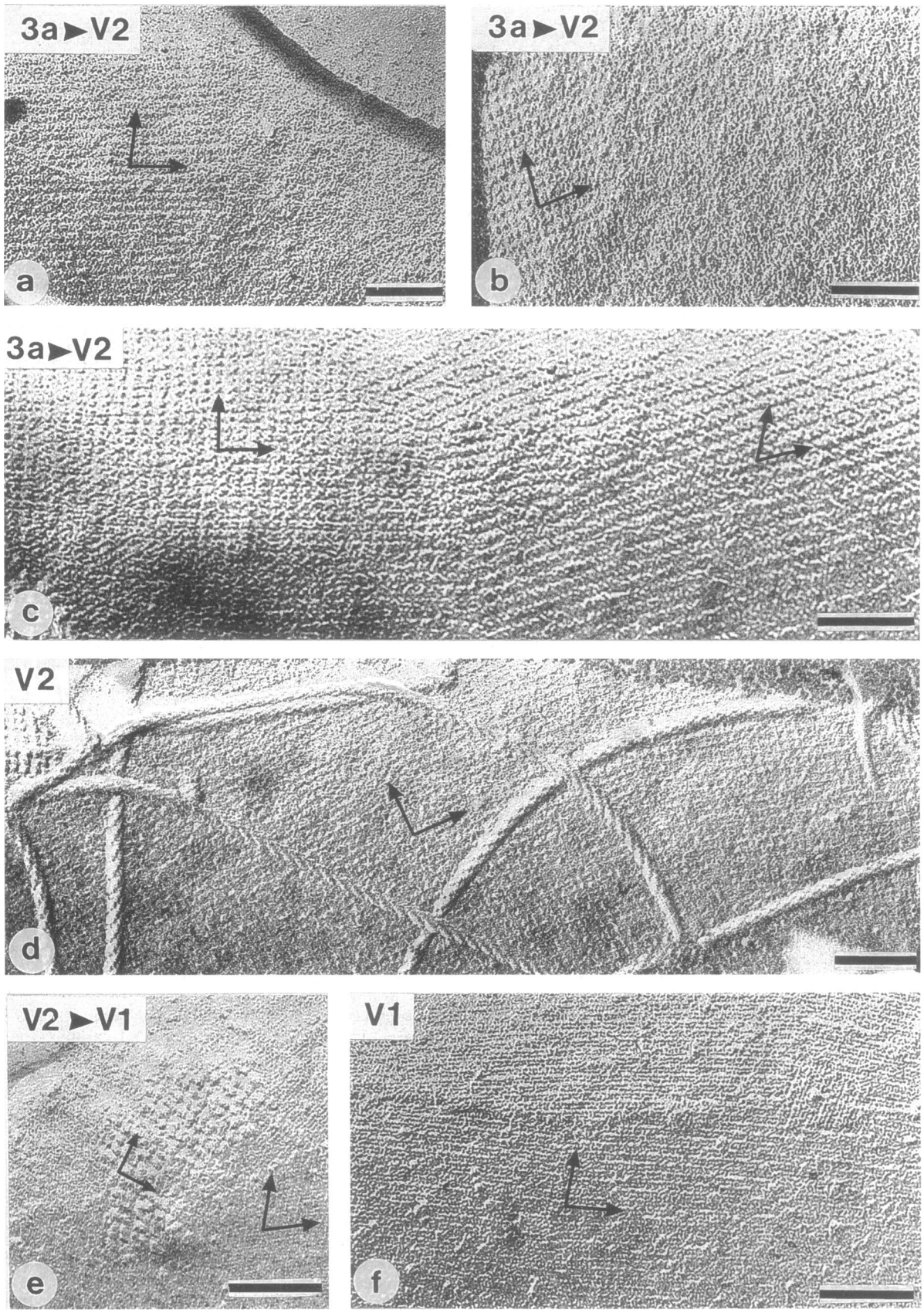
3a►V2
a
3a►V2
b
3a►V2
c
V2
d
V2►V1
e
V1
f

S-layer lattice characteristic of variant 3a/V1, the inoculum was considered homogeneous. When the two variants were grown on SVIII medium in continuous culture under oxygen-limited conditions, acid was produced all the time and the OD_{600} of the suspensions reached a maximum value of 1.5. The production of acid indicated that organisms were restricted to glucose as the sole carbon source. Samples used for SDS-PAGE and freeze-etching confirmed that cultures remained constant during the entire continuous fermentation process, which lasted at least 48 h.

Resistance of whole cells to muramidases. For investigating the resistance of whole cells to lysozyme (M_r, 14,600) and mutanolysin (M_r, 24,000), biomass from the fermentor or cells grown to mid-exponential growth phase in shaking flasks were used. As observed for the wild-type strain (25), both variants were sensitive to the chosen muramidases, indicating that in all S-layer types the pores are large enough for the passage of proteins with molecular weights of at least 24,000.

Self-assembly and image reconstruction. As described in a previous report (26), isolated S-layer subunits from the wild-type strain reassembled into distinct types of cylindrical and sheet-like self-assembly products. The formation of mono- or double-layer self-assembly products correlated with the presence of mono- or bivalent cations during dialysis (26). Isolated S-layer subunits from variant 3a/V1 reassembled both in the absence and presence of mono- or bivalent cations into monolayer sheets (Fig. 5b). As could be demonstrated by negative staining and ultrathin sectioning, the sheet-like and cylindrical self-assembly products from variant 3a/V2 always represented double layers (Fig. 5c and d) which in freeze-dried and Pt-C-shadowed preparations revealed the same surface topography as that observed for freeze-etched intact cells (Fig. 4c). This result indicated that monolayers had bound to each other by their inner S-layer faces.

Upon dialysis of S-layer GHCl extracts containing subunits from the wild-type strain and from variant 3a/V1 or 3a/V2, only amorphous aggregates were formed. This observation that mixtures of S-layer proteins from the wild-type strain and a variant do not lead to crystalline assembly products was in accordance with data from freeze-etching. In the course of switching from the wild-type strain to the variant strains, many irregularly structured areas could be observed on the surfaces of whole cells. As previously demonstrated, a pool of S-layer subunits sufficient for generating at least complete coverage of the cell surface is present in the peptidoglycan-containing layer of *B. stearothermophilus* strains (7). During the transition phase, the pool of S-layer subunits synthesized by the wild-type strain will be mixed with new subunits of the variants. Once liberated on the surface of the peptidoglycan-containing layer, the different types of S-layer subunits are not capable of assembling into separate crystalline domains but rather aggregate into unstructured domains. Only when the subunits of the original S-layer protein are sufficiently diluted by the new protein type can the lattice type characteristic for the variant strain be formed. On the other hand, upon dialysis of mixtures of S-layer GHCl extracts containing subunits from both variants, separate self-assembly products showing either the oblique or square S-layer lattice characteristic of variant 3a/V1 or 3a/V2 formed simultaneously.

Three-dimensional models of the protein mass distribution of the S-layer lattices from the wild-type strain and variant 3a/V2 are shown in Fig. 6. A two-dimensional projection of the S-layer lattice from variant 3a/V1 is given in Fig. 7. The thresholds for the three-dimensional data sets were set so that connectivities between adjacent morphological units were established. On the basis of these preliminary values, a fine tuning of the threshold values was made possible by taking the results from permeability experiments into consideration. The size of the pore was adjusted close to that of carbonic anhydrase (4.1 by 4.1 by 4.7 nm), which had a rejection rate of up to 60%. The apparent thickness of the two three-dimensionally reconstructed S-layer lattices was found to be 7 to 8 nm, as judged from contrast-related maximum-minimum curves in three-dimensional data sets (data not shown) (11). The oblique lattice symmetry from the wild-type strain allowed us to distinguish between the inner and outer faces of three-dimensional reconstructions by comparing the orientations of base vectors with respect to those observed on intact cells (26, 29). The S layer of the wild-type strain had a smooth outer surface and a more corrugated inner surface. The morphological units of the wild-type strain S-layer lattice were composed of a dimer, with the bulk of the protein located around a central twofold axis. The subunits were closely associated along the short base vector and connected by fine arms along the long base vector, yielding a characteristic handedness. The three-dimensional model of the square S-layer lattice from variant 3a/V2 (Fig. 6c and d) revealed a more complicated protein meshwork with no central protein accumulations but a characteristic fourfold handedness. The orientation of the S layer in the three-dimensional data set was determined from ultrathin sections and from freeze-dried preparations of double-layer self-assembly products (not shown) where monolayers had bound to each other by their inner faces as explained above. The different surface topography of monolayer patches extending from the double layer allowed us to distinguish between the inner and outer S-layer faces. The outer face is relatively smooth, while the inner face is strongly corrugated. The characteristic feature of the inner face is large stain-filled cavities with a central pore over a fourfold axis. These cavities appear as dome-shaped protrusions with fourfold symmetry on the inner face. In comparison to Pt-C-shadowed replicas in freeze-dried preparations (not shown), these protrusions are less pronounced in the three-dimensional model, which can be explained by flattening effects during negative staining and radiation damage (11). The protein domains between these protrusions form a typical fourfold cross-like interconnecting structure.

In this study we were not able to determine the space group symmetry of the oblique S-layer lattice from variant 3a/V1. During the phase origin refinement for space group symmetry p2, some low-order reflections such as (2,0), (1, −2), or (3,0) consistently showed phase values of approximately ±90°, while

FIG. 4. Freeze-etched preparations of whole cells harvested at different phases of the continuous culture shown in Fig. 3. During switching from the wild-type strain (Fig. 2a) to variant 3a/V2 (corresponding to samples 2 to 7 in Fig. 3A), the oblique S-layer lattice became interrupted by granular areas (a) and patches of square S-layer lattice appeared on the cell surface (b). Both the oblique lattice from the wild-type strain and the square lattice characteristic of variant 3a/V2 could be detected on a single cell (c). Continuous growth of the culture under high oxygen pressure led to a population of cells covered exclusively with the square S-layer lattice (sample 7 in Fig. 3) (d). With oxygen saturation, variant 3a/V2 switched to variant 3a/V1. In this phase, the square and delicate oblique S-layer lattices characteristic of variant 3a/V1 could be detected on individual cells (e). Finally, in sample stage 9 (Fig. 3) all cells were covered with the oblique S-layer lattice of variant 3a/V1 (f). Bars, 100 nm.

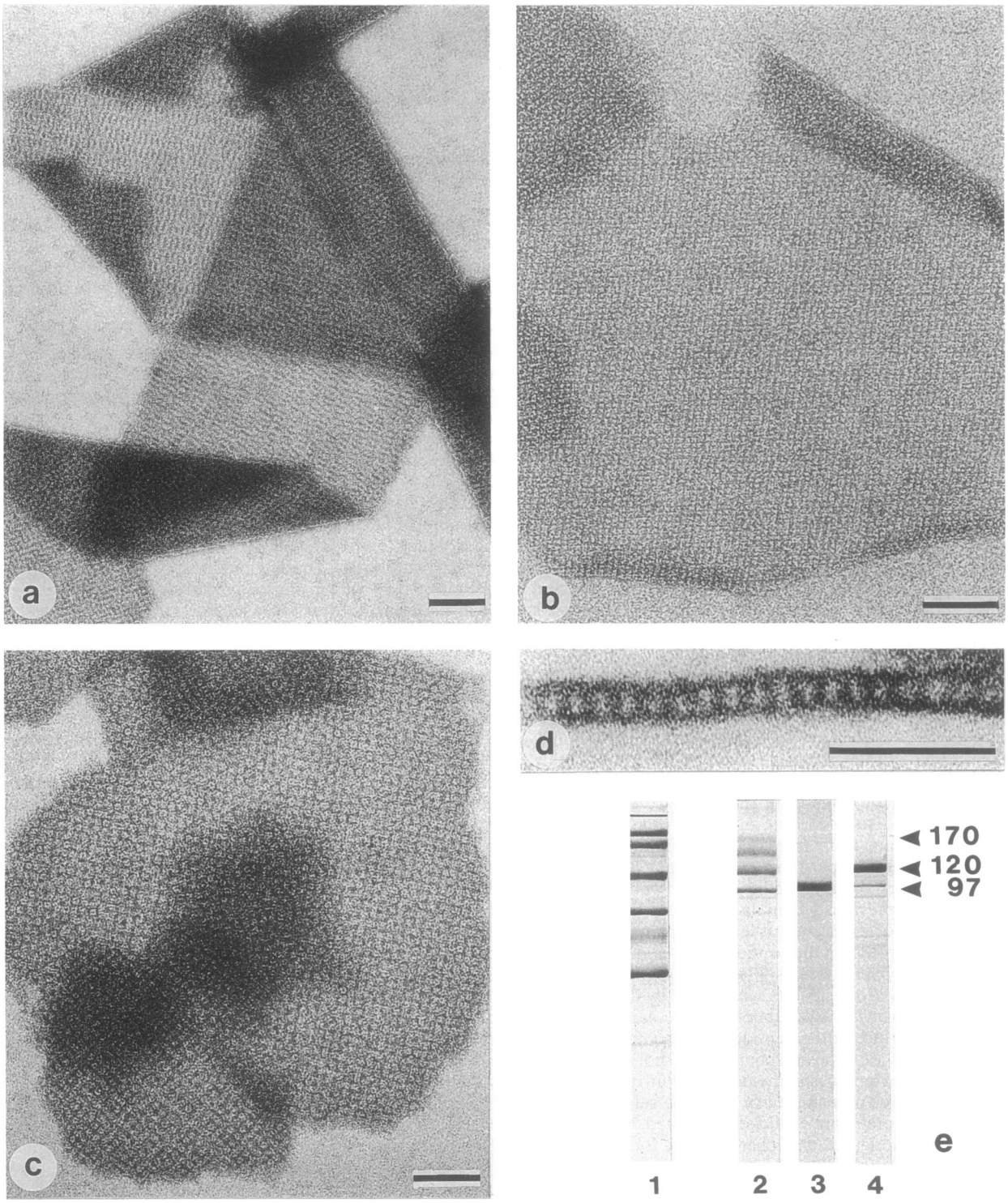

FIG. 5. Negative staining of S-layer self-assembly products from the wild-type strain *B. stearothermophilus* NRS 2004/3a (a) and variants 3a/V1 (b) and 3a/V2 (c). (d) Ultrathin sections from double-layer self-assembly products from 3a/V2 are shown. (e) SDS-polyacrylamide gel electropherograms of the molecular weight standards (lane 1) and the S-layer proteins of the wild-type strain (lane 2), variant 3a/V1 (lane 3), and variant 3a/V2 (lane 4). Values to the right are molecular weights (in thousands). Bars, 100 nm.

all remaining reflections revealed values of either 0 or 180°. The theoretical possibility that values for the monolayer were obscured by a second layer oriented in the same way as the first layer but shifted relative to it could be excluded because this would imply the occurrence of three-dimensional crystallization of the S-layer protein of variant 3a/V1, which has never been observed in this work. On the other hand, because of the oblique symmetry of the S-layer lattice from this variant,

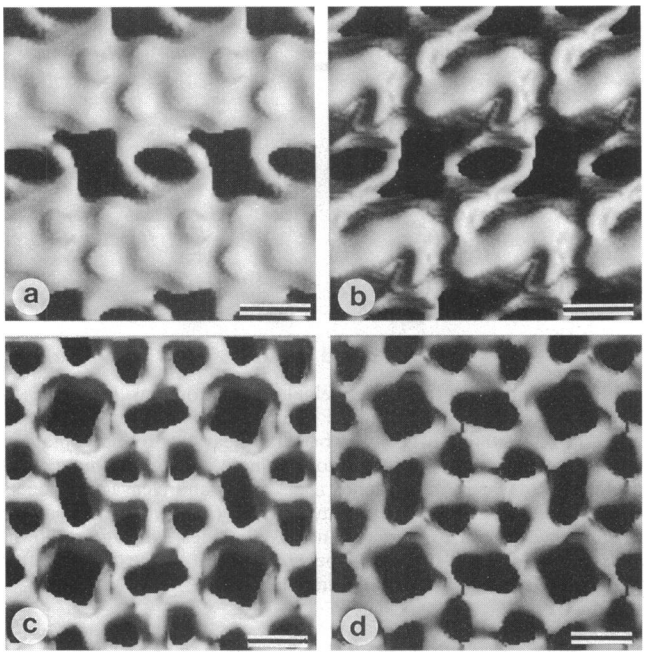

FIG. 6. Three-dimensional models of the protein mass distribution of the S-layer lattice from the wild-type strain *B. stearothermophilus* NRS 2004/3a (a and b) and variant 3a/V2 (c and d). The outer (a and c) and inner (b and d) surfaces are shown. Bars, 5 nm.

double layers which bind to each other either by the inner or outer faces would give two discernible reciprocal lattices. Furthermore, double-layer self-assembly products were never found in ultrathin sections. Finally, it is unlikely that the morphological unit is a monomer, since the molecular weights of the subunits as determined by SDS-PAGE and the size of the unit cell indicate that the unit cell is a dimer. Thus, no symmetry operations were applied to the filtered structure factors of the S-layer lattice of variant 3a/V1. The reconstruction shown in Fig. 7 revealed space group symmetry p1 (primitive). The uncertainty in determining the phase origin could not be resolved by making a three-dimensional model of the S layer (data not shown). Protein accumulates in the center of the unit cells, and pores in the S layer are determined by

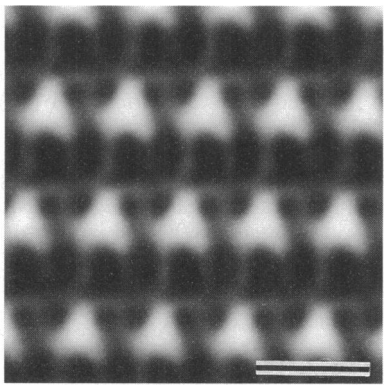

FIG. 7. Two-dimensional projection of the protein mass distribution of the S-layer lattice from variant 3a/V1. Protein is white, and stain is dark. Bar, 10 nm.

TABLE 3. Carbohydrate content of the S-layer proteins from *B. stearothermophilus* NRS 2004/3a and variants 3a/V1 and 3a/V2

Strain and/or growth conditions	Carbohydrate content (% [dry wt]) of S-layer protein			
	Total	Amino sugars	Neutral sugars	Uronic acids
NRS 2004/3a	7.8	0.6	6.1	1.1
3a/V1				
Oxygen saturated	0.5	0.4	0.1	ND[a]
Oxygen limited	4.7	4.2	0.5	ND
3a/V2				
Oxygen saturated	2.1	1.4	0.7	ND
Oxygen limited	4.5	3.7	0.8	ND

[a] ND, not determined.

interconnecting arms. In this unsymmetrized image, reconstruction pores of two distinct sizes could be detected.

Chemical characterization of the S-layer protein from the wild-type strain and the variants. In comparison to the S-layer protein from the wild-type strain, which yielded four bands on SDS-polyacrylamide gels (Fig. 5e, lane 2), the S-layer protein from variant 3a/V1 gave only a single band with an apparent molecular weight of 97,000 (Fig. 5e, lane 3). In all S-layer preparations from variant 3a/V2, a protein band with an apparent molecular weight of 120,000 represented at least 95% of the total protein. Even after purification by column chromatography, a small band with an apparent molecular weight of 97,000 remained. The S-layer protein bands from the variants gave a negative periodate-Schiff reaction.

Carbohydrate analyses of purified S-layer proteins from variants 3a/V1 and 3a/V2 grown under either oxygen-limited or oxygen-saturated growth conditions revealed significant differences in the carbohydrate content from that of the wild-type S-layer protein. Depending on oxygen supply, the total carbohydrate content of the S-layer proteins dropped from about 8% for the wild-type strain (21, 39) to about 4% or less for the variants (Table 3). Remarkably, neither the polyrhamnan (8) nor the diacetamido-dideoxymannuronic acid-containing glycans present in the S-layer protein from the wild-type strain (28) were found in the variants. Instead, glycans containing mainly amino sugars became dominant (Table 4). Generally, under oxygen saturation the carbohydrate content of the S-layer proteins from the variants was significantly lower than under oxygen-limited conditions. Upon switching from oxygen-saturated to oxygen-limited conditions, an increase in the total carbohydrate content from 0.5 to 4.7% was observed for

TABLE 4. Carbohydrates detected in the glycopeptides from the S-layer proteins of variants 3a/V1 and 3a/V2

Variant and growth conditions	Molar ratio of carbohydrate detected from variants 3a/V1 and 3a/V2[a]				Presence of compound X[b]
	Glucosamine	Galactosamine	Glucose	Mannose	
3a/V1	6.3			1.0	–
3a/V2					
Oxygen saturated	3.0	0.3	1.6	1.3	–
Oxygen limited	3.0				+

[a] Mannosamine was set at 1. Amino sugars were quantitated after hydrolysis with 6 N hydrochloric acid for 6 h at 110°C; neutral sugars were quantified after hydrolysis with 2.5 N trifluoroacetic acid for 6 h at 110°C.

[b] X, an unidentified compound that appeared after HCl hydrolysis.

TABLE 5. Amino acid composition of the S-layer proteins from *B. stearothermophilus* NRS 2004/3a (wild type) and variants 3a/V1 and 3a/V2

Amino acid	Amino acid composition (mol%) of S-layer protein from strain:		
	NRS2004/3a	3a/V1	3a/V2
Asx	14.1	12.3	12.6
Thr	9.0	8.9	9.3
Ser	6.5	5.6	5.5
Glx	8.7	9.3	9.8
Pro	2.8	3.3	2.8
Gly	5.2	7.3	9.4
Ala	11.8	10.3	12.2
Val	10.4	9.9	10.4
Met	0.5	1.3	0.5
Ile	3.8	4.3	3.6
Leu	6.5	6.0	5.0
Tyr	3.8	3.6	3.2
Phe	3.5	4.3	3.9
His	0.8	1.0	0.8
Lys	9.8	9.3	8.9
Arg	2.8	3.3	2.5

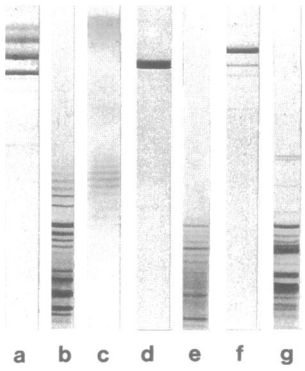

FIG. 8. SDS-polyacrylamide gel electropherograms from the S-layer proteins from the wild-type strain from *B. stearothermophilus* NRS 2004/3a and the variants and from the cleavage products obtained after peptide mapping with endoproteinase Glu-C (*S. aureus* V8 protease). S-layer proteins (lanes a, d, and f) and cleavage products (lanes b, e, and g) from the wild-type strain (lanes a and b), variant 3a/V1 (lanes d and e), and variant 3a/V2 (lanes f and g) reshown. Glycopeptides from the wild-type strain were made visible after blotting to nitrocellulose membranes (lane c).

variant 3a/V1 (Table 3). As shown in Table 4, the molar ratio of the constituting sugars remained constant. By contrast, for variant 3a/V2, the increase in total carbohydrate content of the S-layer protein upon reducing oxygen supply was accompanied by a considerable decrease in the amount of neutral sugars and the loss of galactosamine (Table 4). Also, an unknown substance designated X which was not observed in glycopeptides derived from oxygen-saturated cultures appeared. Because of the absence of suitable reference compounds, identification of this component was not possible. Amino acid compositions of the different S-layer proteins are given in Table 5. With the exception of glycine, which was present in the S-layer protein from variant 3a/V2 in a significantly higher amount than in the S-layer protein from the wild-type strain, the amino acid compositions of the three S-layer proteins were rather similar and typical for members of the family *Bacillaceae* (36). Peptide mapping using endoproteinase Glu-C (*S. aureus* V8 protease, which specifically attacks proteins after Asp and Glu residues) yielded quite different cleavage products, even for the minor glycosylated S-layer proteins from the variants (Fig. 8). This result indicated that the S-layer proteins from the wild-type strain and the variants have different amino acid sequences. For the S-layer glycoprotein from the wild-type strain, five distinct glycopeptide bands with apparent molecular weights of 40,000, 42,000, 43,000, 45,000, and 47,000 could be visualized after blotting to nitrocellulose membranes (Fig. 8c). It could be also demonstrated that the S-layer proteins from the wild-type strain and the variants possess different N-terminal amino acid sequences. The following N-terminal regions were obtained: Ala-Thr-Asp-Val-Ala-Thr-Val-Val-Ser-Gln-Ala-Lys-Ala-Gln-Met for the wild-type strain, Ala-Ser-Phe-Thr-Asp-Val-Ala-Pro-Gln-Tyr-Lys-Asp-Ala-Ile for variant 3a/V1, and Ala-Ser-Phe-Thr-Asp-Leu-Ala-Gly-Ser-Val-His-Ala-Asp-Ala for variant 3a/V2. All sequences indicate that S-layer proteins were synthesized with a signal sequence which was processed from mature proteins. Interestingly, the first five amino acids from the N-terminal regions of the S-layer proteins from the variants were identical and could represent small conserved domains.

Permeability studies on S-layer membranes. As shown by permeability studies applying the S-layer membrane technique, S layers from the wild-type strain and both variants allowed free passage for myoglobin with a molecular weight of 17,000 (Table 6) but rejected ovalbumin (M_r, 43,000) and bovine serum albumin (M_r, 67,000). Sixty percent of the carbonic anhydrase, with a molecular weight of 30,000 and a molecular size of 4.1 by 4.1 by 4.7 nm, was rejected by the oblique S-layer lattice of the wild-type strain and the square S-layer lattice of variant 3a/V2. In contrast, the oblique S-layer lattice from variant 3a/V1 rejected only 20% of carbonic anhydrase molecules (Table 6).

DISCUSSION

The original properties of the S-layer glycoprotein from *B. stearothermophilus* NRS 2004/3a could be preserved in continuous culture on complex medium in oxygen-limited conditions only if glucose was the sole carbon source. Upon relieving oxygen limitation, amino group-containing compounds were also metabolized, which was expressed in the liberation of ammonium. The observed changes in the physiology of the culture were always linked to irreversible but absolutely reproducible changes in the S-layer glycoprotein. Depending on the phase of fermentation at which the oxygen supply was increased, either variant 3a/V1 or variant 3a/V2 could develop. With increased oxygen supply, variant 3a/V2 switched to variant 3a/V1, which was the most stable form under conditions of stronger aeration.

Similar observations of spontaneous changes of S-layer proteins were reported for *B. sphaericus* P-1 (16) and for the

TABLE 6. Percent rejection of test proteins by the S-layer lattice from the wild-type strain *B. stearothermophilus* NRS 2004/3a and variants 3a/V1 and 3a/V2

Test protein (mol wt)	% Rejection of test proteins through S-layer lattice of strain:		
	NRS 2004/3a	3a/V1	3a/V2
Myoglobin (17,000)	5	0	0
Carbonic anhydrase (30,000)	60	20	60
Ovalbumin (43,000)	>95	>95	>95
Bovine serum albumin (67,000)	>98	>98	>98

pathogen *Campylobacter fetus* (13). For *B. sphaericus* P-1 only changes in the molecular sizes of the S-layer subunits were observed, whereas for *C. fetus* an alteration in the molecular sizes of S-layer subunits was associated with changes in antigenicity and lattice type. The S-layer proteins of larger molecular size assembled into square lattices, whereas those of smaller molecular size formed hexagonally ordered arrays. With *C. fetus* it was also shown for the first time that during the switching phase from the parent strain to the variant strains two types of S-layer lattices with different symmetry can exist as a monomolecular layer on single cells (13). This was also observed in the present study for *B. stearothermophilus* NRS 2004/3a, where during the switching phase from one S-layer protein to another, two different lattice types were arranged on the surfaces of single cells in a monomolecular layer. In contrast to *C. fetus*, in which the N-terminal regions represented a highly conserved domain (13), the S-layer proteins investigated in this study showed completely different N-terminal sequences. This observation and the data from peptide mapping showing that quite different cleavage products are formed even for the minor glycosylated S-layer proteins from the variants strongly indicate that the three S-layer proteins are encoded by different genes and are not processed from a universal precursor form.

Many of the *B. stearothermophilus* strains were originally isolated from extraction plants in beet sugar factories where they grew in an environment rich in sugar, amino acids, peptides, salts, and vitamins. Because of the temperature and viscosity of the system and the small area at which interactions between air and liquid can occur, bacteria will be supplied with a minimum of oxygen. It can be generally assumed that because of the low solubility of oxygen at elevated temperatures, the growth conditions for thermophilic bacteria in their natural habitats will be quite different from those generated in a fermentor with a high aeration rate. It seems that excess oxygen leads to a situation where after respiration of sugars, which represent the preferred carbon source for *B. stearothermophilus* strains, the cell's metabolism is reorganized for oxidative degradation of additional substrates such as amino acids.

Although the biological function of S layers from thermophilic members of the family *Bacillaceae* is still unknown, it can be assumed that similar to other cell surface components (9), they endow the living cell with a selective advantage in competitive habitats (27). Therefore, it is not surprising that under conditions lacking a selection pressure, the properties of the outermost cell surface layer change. As has been observed for exopolysaccharides constituting typical glycocalices (9), the carbohydrate composition of the S-layer protein from *B. stearothermophilus* NRS 2004/3a was also influenced by changing growth conditions. The S-layer proteins from the variant strains which had developed in noncompetitive environments and with a higher aeration rate had a significantly lower carbohydrate content and lacked the polyrhamnan chain and the uronic acid-containing glycans characteristic of the wild-type strain. Although the three S-layer proteins from the wild-type strain and variants revealed comparable amino acid compositions and very similar permeability properties for selected test molecules, the possibility that switching from one S-layer protein to another is linked to considerable changes in the arrangement of charged, hydrophilic, and hydrophobic groups in the three-dimensional protein network cannot be excluded. Such alterations in the physicochemical properties of the S-layer surface and the pore areas would allow quite different interactions between the cells and materials in the environment and nutrients. It is interesting that the S-layer protein from variant 3a/V1, which was the most stable form under optimal laboratory conditions, had the simplest lattice structure.

ACKNOWLEDGMENTS

This work was supported by the Fonds zur Förderung der Wissenschaftlichen Forschung in Österreich (projects S50/02, S57105, and P8922-MOB), by the Jubiläumsstiftung der Österreichischen Nationalbank (project 4332), and by the Österreichisches Bundesministerium für Wissenschaft and Forschung.

We thank Irina Ciuca, Harald Mayer, Andrea Scheberl, and Sonja Zayni for technical assistance. We also thank Karola Vorauer-Uhl for N-terminal sequencing.

REFERENCES

1. **Amartey, S. A., D. J. Leak, and B. S. Hartley.** 1991. Effects of temperature and medium composition on the ethanol tolerance of *Bacillus stearothermophilus* LLD-15. Biotechnol. Lett. **13**:627–632.
2. **Amos, L., R. Henderson, and P. N. T. Unwin.** 1982. Three-dimensional structure determination by electron microscopy of two-dimensional crystals. Prog. Biophys. Mol. Biol. **39**:183–231.
3. **Bartelmus, W., and F. Perschak.** 1957. Schnellmethode zur Keimzahlbestimmung in der Zuckerindustrie. Z. Zuckerind. **7**:276–281.
4. **Baumeister, W., and H. Engelhardt.** 1987. Three-dimensional structure of bacterial surface layers, p. 109–154. *In* J. R. Harris and R. W. Horne (ed.), Electron microscopy of proteins, vol. 6. Membraneous structures. Academic Press Ltd., London.
5. **Beveridge, T. J., and L. L. Graham.** 1991. Surface layers of bacteria. Microbiol. Rev. **55**:684–705.
6. **Beveridge, T. J., and S. F. Koval (ed.).** 1993. Advances in bacterial paracrystalline surface layers. Plenum Press, New York.
7. **Breitwieser, A., K. Gruber, and U. B. Sleytr.** 1992. Evidence for an S-layer protein pool in the peptidoglycan of *Bacillus stearothermophilus*. J. Bacteriol. **174**:8008–8015.
8. **Christian, R., G. Schulz, F. M. Unger, P. Messner, Z. Küpcü, and U. B. Sleytr.** 1986. Structure of a rhamnan from the surface layer glycoprotein of *Bacillus stearothermophilus* strain NRS 2004/3a. Carbohydr. Res. **150**:265–272.
9. **Costerton, J. W., T. J. Marrie, and K. J. Cheng.** 1985. Phenomena of bacterial adhesion, p. 3–43. *In* D. C. Savage and M. Fletcher (ed.), Bacterial adhesion. Mechanisms and physiological significance. Plenum Press, New York.
10. **Dagley, S.** 1978. Pathways for the utilization of organic growth substrates, p. 305–388. *In* I. C. Gunsalus (ed.), The bacteria, vol. VI. Bacterial diversity. Academic Press, Inc., New York.
11. **Engelhardt, H.** 1988. Correlation averaging and 3-D reconstruction of 2-D crystalline membranes and macromolecules. Methods Microbiol. **20**:357–413.
12. **François, C., D. Marshall, and A. Neuberger.** 1962. Carbohydrates in protein: determination of mannose in hen's-egg albumin by radioisotope dilution. Biochem. J. **83**:335–341.
13. **Fujimoto, S., A. Takade, K. Amako, and M. J. Blaser.** 1991. Correlation between molecular size of the surface array protein and morphology and antigenicity of the *Campylobacter fetus* S layer. Infect. Immun. **59**:2017–2022.
14. **Haselbeck, A., and W. Hösel.** 1990. Description and application of an immunological system for analyzing glycoproteins on blots. Glycoconjugate J. **7**:63–74.
15. **Hovmöller, S., A. Sjögren, and D. N. Wang.** 1988. The structure of crystalline bacterial cell surface layers. Prog. Biophys. Mol. Biol. **51**:131–163.
16. **Howard, L., and D. J. Tipper.** 1973. A polypeptide bacteriophage receptor: modified cell wall protein subunits in bacteriophage-resistant mutants of *Bacillus sphaericus* strain P-1. J. Bacteriol. **113**:1491–1504.
17. **Jurado, A. S., A. C. Santana, M. S. da Costa, and V. M. C. Madeira.** 1987. Influence of divalent cations on the growth and morphology of *Bacillus stearothermophilus*. J. Gen. Microbiol. **133**:507–513.
18. **König, H.** 1988. Archaeobacterial cell envelopes. Can. J. Microbiol. **34**:395–406.

19. **Koval, S. F.** 1988. Paracrystalline protein surface arrays on bacteria. Can. J. Microbiol. **34:**407–414.
20. **Kübler, O.** 1980. Unified processing of periodic and nonperiodic specimens. J. Microsc. Spectrosc. Electron. **5:**561–575.
21. **Küpcü, Z., L. März, P. Messner, and U. B. Sleytr.** 1984. Evidence for the glycoprotein nature of the crystalline cell wall layer of *Bacillus stearothermophilus* strain NRS 2004/3a. FEBS Lett. **173:** 185–190.
22. **Laemmli, U. K.** 1970. Cleavage of structural proteins during the assembly of the head of bacteriophage T4. Nature (London) **227:**680–685.
23. **Martins, M. L. L., and D. W. Tempest.** 1991. Metabolic response of *Bacillus stearothermophilus* chemostat culture to a secondary oxygen limitation. J. Gen. Microbiol. **137:**1391–1396.
24. **Messner, P., R. Christian, J. Kolbe, G. Schulz, and U. B. Sleytr.** 1992. Analysis of a novel linkage unit of O-linked carbohydrates from the crystalline surface layer glycoprotein of *Clostridium thermohydrosulfuricum* S102-70. J. Bacteriol. **174:**2236–2240.
25. **Messner, P., F. Hollaus, and U. B. Sleytr.** 1984. Paracrystalline cell wall surface layers of different *Bacillus stearothermophilus* strains. Int. J. Syst. Bacteriol. **34:**202–210.
26. **Messner, P., D. Pum, and U. B. Sleytr.** 1986. Characterization of the ultrastructure and the self-assembly of the surface layer of *Bacillus stearothermophilus* strain NRS 2004/3a. J. Ultrastruct. Mol. Struct. Res. **97:**73–88.
27. **Messner, P., and U. B. Sleytr.** 1992. Crystalline bacterial cell-surface layers. Adv. Microb. Physiol. **33:**213–275.
28. **Messner, P., U. B. Sleytr, R. Christian, G. Schulz, and F. M. Unger.** 1987. Isolation and structure determination of a diacetamidodideoxymannuronic acid-containing glycan chain from the S-layer glycoprotein of *Bacillus stearothermophilus* NRS 2004/3a. Carbohydr. Res. **168:**211–218.
28a. **Pharmacia LKB.** 1991. Application note 348. Pharmacia LKB, Lund, Sweden.
29. **Pum, D., M. Sára, and U. B. Sleytr.** 1989. Structure, surface charge, and self-assembly of the S-layer lattice from *Bacillus coagulans* E38-66. J. Bacteriol. **171:**5296–5303.
30. **Rondle, C. J. M., and W. T. J. Morgan.** 1955. The determination of glucosamine and galactosamine. Biochem. J. **61:**586–589.
31. **Sára, M., D. Pum, and U. B. Sleytr.** 1992. Permeability and charge-dependent adsorption properties of the S-layer lattice from *Bacillus coagulans* E38-66. J. Bacteriol. **174:**3487–3493.
32. **Sára, M., and U. B. Sleytr.** 1987. Molecular sieving through S layers of *Bacillus stearothermophilus* strains. J. Bacteriol. **169:** 4092–4098.
33. **Sára, M., and U. B. Sleytr.** 1987. Production and characteristics of ultrafiltration membranes with uniform pores from two-dimensional arrays of proteins. J. Membr. Sci. **33:**27–49.
34. **Saxton, W. O.** 1985. Computer generation of shaded images of solids and surfaces. Ultramicroscopy **16:**387–394.
35. **Sleytr, U. B., and A. M. Glauert.** 1975. Self-assembly of the hexagonally and tetragonally arranged subunits of bacterial surface layers and their reattachment to cell walls. J. Ultrastruct. Res. **55:**360–377.
36. **Sleytr, U. B., and P. Messner.** 1983. Crystalline surface layers on bacteria. Annu. Rev. Microbiol. **37:**311–339.
37. **Sleytr, U. B., and P. Messner.** 1988. Crystalline surface layers in procaryotes. J. Bacteriol. **170:**2891–2897.
38. **Sleytr, U. B., P. Messner, D. Pum, and M. Sára (ed.).** 1988. Crystalline bacterial cell surface layers. Springer, Berlin.
39. **Sleytr, U. B., M. Sára, Z. Küpcü, and P. Messner.** 1986. Structural and chemical characterization of S-layers of selected strains of *Bacillus stearothermophilus* and *Desulfotomaculum nigrificans*. Arch. Microbiol. **146:**19–24.
40. **Sonnleitner, B.** 1983. Biotechnology of thermophilic bacteria—growth, products and application. Adv. Biochem. Eng. Biotechnol. **28:**69–138.
41. **Sorensen, S. B., T. L. Sorensen, and K. Breddam.** 1991. Fragmentation of proteins by *S. aureus* strain V8 protease. FEBS Lett. **294:**195–197.
42. **Wolf, J., and R. J. Sharp.** 1981. Taxonomic and related aspects of thermophiles within the genus *Bacillus*, p. 251–296. *In* R. C. W. Berkeley and M. Goodfellow (ed.), The aerobic endospore-forming bacteria: classification and identification. Academic Press, Inc., New York.